Academic Science Journal

Influence Laser Energies on the Structural, Optical and Electrical Properties of Cds Nps by Pulsed Laser Ablation in Distilled Water

Yamamah K. Abdalaah[1*], Olfat A. Mahmood[1] and Suaad S. Shaker[2]

[1]Department of Physics, College of Science, University of Diyala

[2]Department of Applied Science, University of Technology, Baghdad, Iraq.

[*]yamamahkhaled89@gmail.com.

Received: 27 August 2023 **Accepted: 16 October 2023**

DOI: https://dx.doi.org/10.24237/ASJ.02.04.803C

Abstract

The influence of laser energies on the: structural, optical, morphological, and electrical properties of CdS nanoparticles was studied using X-ray diffraction (XRD), UV–vis spectroscopy, Field Emission Scanning Electron Microscope (FE-SEM), Fourier Transform Infrared Spectroscopy (FTIR), and Hall measurement. The XRD data indicate that synthesized CdS nanoparticles are nanocrystalline and possess a hexagonal wurtzite structure. The calculated lattice constants of CdS nanostructures are (a = 4.105), (c = 6.662), and c/a=1.622. The direct optical energy gap of CdS was determined to be between 2.42 and 1.71 eV, depending on the laser energy. In the CdS colloidal solution. In FT-IR spectra, the Cd–S stretching frequency is detected in the wave number region below 700 cm-1. Electrical analysis revealed that the synthesized CdS NPs were n-type with mobility increasing with laser energy 530, 590 mJ and decreasing with laser energy 650 mJ. The I-V characteristics of (n-CdS NPs/p-Si) display that the current increased exponentially with increasing voltage, whereas at reverse bias, the current increased slowly with increasing voltage.

Keywords: CdS NPs, PLAL, Optical, Structure and Electrical properties.

Academic Science Journal

تأثير طاقة الليزر على الخصائص البصرية والتركيبية والكهربائية لجسيمات CdS النانوية بواسطة الاستئصال بالليزر النبضي في الماء المقطر

يمامه خالد عبدالله[1], الفت احمد محمود[1], سعاد سالم شاكر[2]

[1]قسم الفيزياء - كلية العلوم - جامعة ديالى

[2] قسم العلوم التطبيقية - الجامعة التكنولوجية

الخلاصة

تمت دراسة تأثير طاقات الليزر على الخصائص التركيبية والبصرية والمورفولوجية والكهربائية للجسيمات النانوية CdS باستخدام: حيود الأشعة السينية (XRD) ، التحليل الطيفي للأشعة المرئية وفوق البنفسجية ، والمجهر الإلكتروني لمسح الانبعاث الميداني (FE-SEM) ، مطيافية فوريه لتحويل الأشعة تحت الحمراء (FTIR) ، وقياس (Holl). تشير بيانات XRD إلى أن الجسيمات النانوية CdS المُصنَّعة عبارة عن جزيئات نانوية بلورية وتمتلك بنية سداسية الشكل من wurtzite ، وقد تم حساب الثوابت الشبكية للبنى النانوية CdS لتكون ((a = 4.105، c = 6.662)) ، و c / a = 1.622. تم تحديد فجوة الطاقة الضوئية المباشرة لـ CdS بين 2.42 و 1.71 الكترون فولت ، اعتمادًا على طاقة الليزر. في أطياف FT-IR ، يتم الكشف عن تردد التمدد Cd-S في منطقة رقم الموجة التي تقل عن $700\ cm^{-1}$. أظهر التحليل الكهربائي أن الجسيمات النانوية CdS المُصنَّعة كانت من النوع n مع زيادة الحركة مع طاقة الليزر 530 ، 590 مللي جول وتتناقص مع طاقة الليزر 650 مللي جول. توضح خصائص I-V لـ (n-CdS NPs / p-Si) أن التيار زاد بشكل كبير مع زيادة الجهد ، بينما في التحيز العكسي ، زاد التيار ببطء مع زيادة الجهد.

الكلمات المفتاحية: جسيمات CdS النانوية, الأستئصال بالليزر النبضي, الخصائص البصرية والتركيبية والكهربائية

Introduction

Nanotechnology is defined as the manipulation of matter with at least one dimension scaled between 1 and 100 nanometers (nm), and concentrates on materials with length scales within the nanometer range [1]. In nanoparticles (NPs), the increased proportion of atoms at the grain boundaries results in a larger specific volume (surface-to-volume ratio), which in turn results in novel optical, catalytic, and electrical properties [2]. Nanoparticles' unique characteristics make them useful in a wide various of nanotechnology applications, including nano-photonics devices, drug delivery, solar cells, catalysis, sensors, and nano-textiles [3]. The inorganic chemical with the formula CdS is cadmium sulfide. Due to its direct and broad optical band gap (2.42 eV) at ambient temperature, it is considered one of the most desirable II and VI semiconductors. It is a stable substance with optical absorption at 515 nm that enables emission

in the visible spectrum. [4,5]. CdS possesses two distinct crystal structures: wurtzite and zinc mix figure (5). Wurtzite is the most stable and easily synthesized phase; it is observed in bulk and nanostructure. Zinc mix is a metastable phase that transitions to a hexagonal phase between 20 and 900 $\overset{o}{c}$ and is exclusively detected in nanostructures [6]. CdS can be mixed with other layers for usage in some types of solar cells when it is in thin-film form [7]. CdS was also among the first semiconductor materials utilized for thin-film transistors (TFTs). Pulsed laser ablation in liquids (PLAL) is the most recent method for producing nanoparticles compared to other methods, and it has garnered a great deal of attention as an innovative NP production method [8]. The PLAL process is a technique to produce NPs physically and does not involve any chemical reaction in the synthesis of NPs. It is environmentally friendly because there is no emission of hazardous and toxic gases [8]. The resultant nanoparticles and colloidal solutions are ultrapure (they do not contain any counterions or reaction by-products), which facilitates their use in biological or biochemical in vivo applications. This technique yields nanoparticles in the form of a colloidal suspension, which increases safety compared to dry-processed nanoparticles [8,9]. Different parameters, such as laser wavelength, laser energy, number of laser pulses, type of colloid solution, and pulse time, can influence the characteristics of synthesized nanoparticles using this method. In this paper, we describe the production of CdS nanoparticles by ablation of a CdS target with a Nd:YAG laser in distilled water. In addition, the effect of laser energy on the properties of nanoparticles was proven and compared to previously published findings.

Experimental Work

99.9% pure powder of cadmium sulfide (CdS) was used to prepare the target. 5 g of CdS were placed in a one-sided pressing mold using a hydraulic press under a press 6 ton to produce 1 cm-diameter pellet of CdS, (CdS) nanoparticle suspension was produced by the pulsed 'laser ablation of CdS pellet in the bottom of a glass vessel with 2 ml of distilled water (DW) above the target and the distance between the solid target and the laser lens was approximately (10 cm). The creation of colloidal (CdS NPs) was accomplished under normal conditions (pressure and temperature) using 300 pulses and three distinct laser energies (530, 590, and 650 mJ) at a laser wavelength of 1064 nm and a laser frequency of (1 Hz). Using a spectrophotometer

(model-Shimadzu, 1800) with a double beam of (UV-VIS) at room temperature, the absorption spectra of the (CdS) NPs solution under various conditions were analyzed in the spectral region of (190-1100 nm). The solutions were placed in quartz cells (optical path equal 1 cm). The optical characteristics of the (CdS) NPs colloids were then determined. The optical energy band gap and absorption coefficient are computed using the wavelength absorbance output data in the program (OriginLab 8.5). The Photoluminesces was examined using (ELICO,SL174, Specetrophotometer, Xe LAMP Power Supply) (PL). Photoluminescence is a physical phenomenon that is employed to study the electronic structure of matter. The external source was employed to excite the electronic state, which then released energy in the form of light. The information from PL was used to calculate the various importation characteristics, including band gap determination. In PL measurements, the wavelength range was around (200-900) nm.

Structure and crystallinity of nanoparticles were analyzed using an X-ray diffractometer (XRD, SHIMADZU, 6000). The structure of nanoparticles was examined using a Field Emission Scanning Electron Microscope (FE-SEM) (MIRA3 model-TE-SCAN). By evaluating the groups and bands in the infrared spectrum, FTIR type (IRAFFINITY-1) was utilized to determine the type of bonds between the resultant compound (CdS) in the range (400-4000) cm^{-1}.

Results and Discussions

a. Optical Properties

Fig. 1 illustrates the absorption spectra of CdS NPs colloidal solution prepared at various laser energy (530, 590, and 650) mJ and laser pulse counts (300). It is evident that the absorbance of CdS NPs colloidal solution decreases dramatically beyond 330 nm and tends to reach saturation at 600 nm. Absorbance decreases at long wavelengths (low energies) correlating to the energy gap (when the incident photon has an energy equal to or less than the energy gap value). Physically, this indicates that the incident photon was powerful enough to agitate the electron and shift it from the valence band to the conduction band since the photon's energy is larger than the energy gap of the semiconductor. Based on absorption data near the fundamental absorption edge, the absorption coefficient (α) can be calculated as follows:

Academic Science Journal

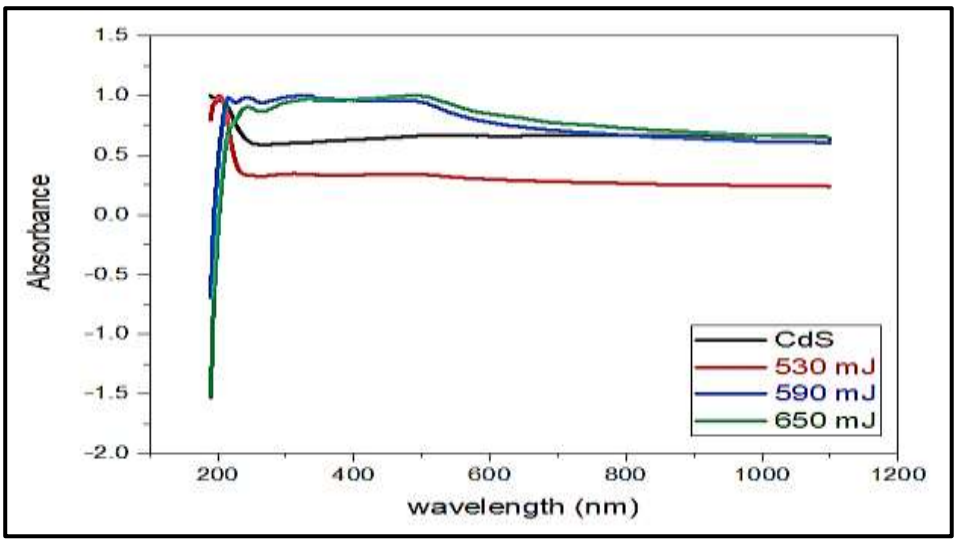

Figure 1: Absorbance versus wavelength of CdS NPs prepared with different laser energies

$\alpha = (1/t)\ Ln\ (1/T)$ …….(1)

where: T is the transmittance , t is the thickness. Using Tauc's relationship, we determined the energy gap E_g of CdS nanoparticles [10]:

$\alpha h\nu = A(h\nu - E_g)^{1/2}$ ……(2)

where: A is a constant , hν is the energy of a photon. The energy gap of CdS nanoparticles was calculated using the plot of $(ah\nu)^2$ versus (hν), where the intercept of the straight line with the hν axis represents the band gap. High laser energy increases the laser radiation intensity delivered to the target, hence increasing the number of NPs with a smaller size and, consequently, the optical band gaps, depicted in Figure (2). The value of CdS nanoparticles' direct optical energy gap was determined to be (2.42 ev). The band gap of CdS ablated NPs decreases from 2.31 to 1.71 ev at laser energies are increases from 530 to 650 mJ due to the high density of NPs ablated that cover the surface of the target and absorbing the energy of the incident laser beam and reducing the band gap of the produced.

Academic Science Journal

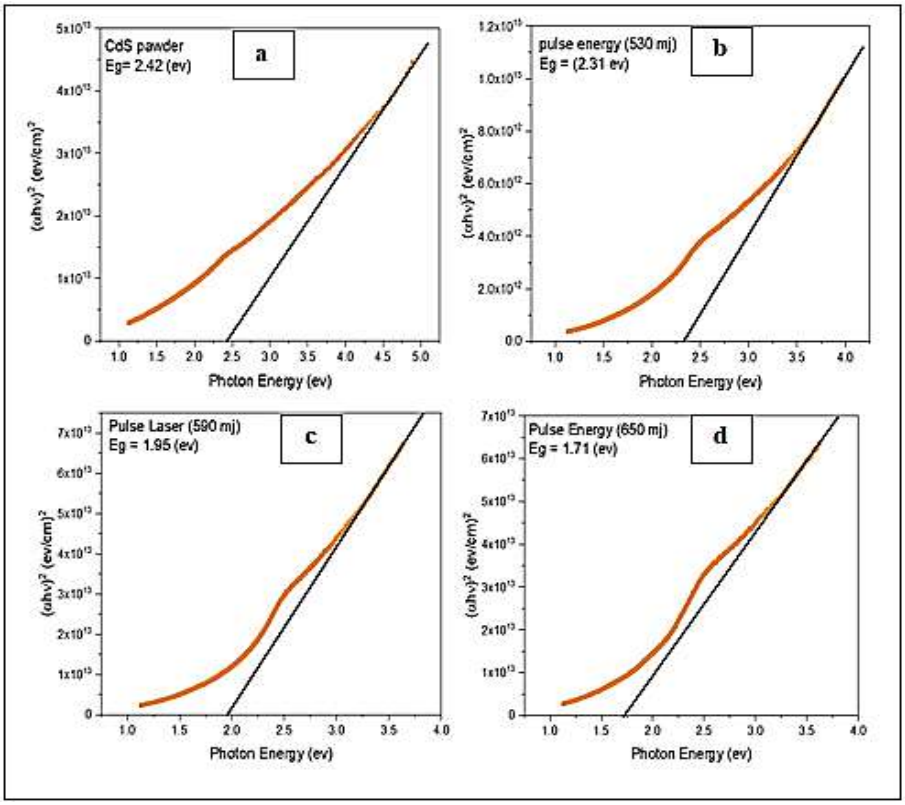

Figure 2: Direct energy gap for CdS NPs synthesized with various laser energies: (a) pawder, (b) 530 mJ, (c) 590 mJ, (d) 650 mJ

Figure (3) illustrates the Photoluminescence spectra (PL) of CdS nanostructures colloidally produced with various laser energies. PL spectra display broad peaks at approximately 500.095 nm (black emission 530 mJ) corresponding to (2.47952 eV) and 500.006 nm (red emission 590 mJ) corresponding to (2.47997 eV), This may be owing to the presence of trapping states in the band gap of CdS, which is not in accordance with optical absorption data. [11]. And (blue emission) corresponds to (2.47995 eV) when the laser energy is 650 mJ. After raising the laser's power, no significant change in PL emission was seen. With increasing laser energy, the PL intensity was shown to increase. Increasing the laser energy from 530 to 650 mJ also enhanced the FWHM of PL emission. The broadening of PL peaks at high laser energies is likely the result of non-radiative and radiative recombination caused by particle agglomeration, size distribution, and structural flaws.

Academic Science Journal

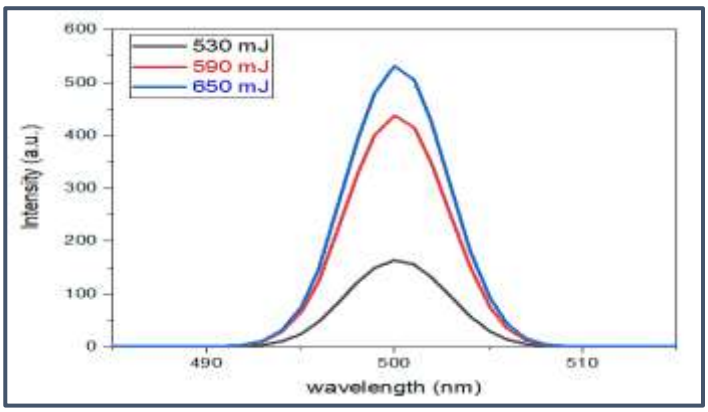

Figure 3: PL spectra of (CdS) nanostructures colloidal synthesized at various laser energy.

b. Structure Properties

XRD analysis in figure (4) for the Cadmium Sulfide (CdS) nanoparticles given showed that (CdS) has a polycrystalline hexagonal structure according to JCPDS card (no:41-1049) with different orientations (002), (110) and (112) and with preferred orientation in (002) direction with 2θ = (26.74, 44.074 and 52.087). From (2θ = 26.74° and 44.074°), the lattice constants of CdS nanostructures were calculated to be (a = 4.105), (c = 6.662), and c/a=1.622. These results resemble those reported in the literature [12]. Using the formula of Debye-Scherrer, the average crystallite size (D_{av}) can be computed [13]:

$$\mathbf{D_{av} = K \lambda / \beta \cos\theta \quad \ldots\ldots\ldots(3)}$$

Where K: is constant, which is dependent on the material's shape, and its value within the range (0.9-1). β: Full Width Half Maximum (FWHM), is measured in radians. θ: Angle of Bragg diffraction. λ: the wavelength of the X-rays that hit the target.

The average size of hexagonal crystallites was determined. Scherrer's formula yields D_{av} values of (3.69, 3.44, 3.43, and 3.26) nm for CdS powder and laser energies of 530, 590, and 650 mJ, respectively. Dislocation density and the strain for CdS NPs generated on the film were calculated using equations:

$$\mathbf{\delta = 1/ (D^2_{av}) \quad \ldots\ldots\ldots(4)}$$

$$\mathbf{\varepsilon = (\beta \cos \theta) / 4 \ldots\ldots\ldots(5)}$$

Where: (δ) is Dislocation density, (ε) is strain.

P-ISSN: 2958-4612
E-ISSN: 2959-5568

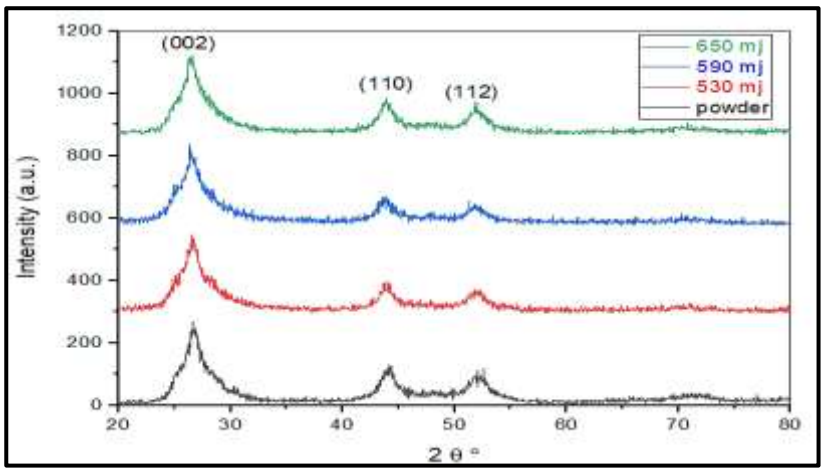

Figure 4: X-Ray patterns of CdS nanoparticles synthesized at various laser energies

The strain and dislocation density depended on laser energy and The FWHM of a long reflection (002) plane of CdS, as shown in tables (1).

Table 1: XRD results for FWHM, Crystallite size, dislocation density, and strain of CdS NPs for preferred orientation (002) at various laser energies.

Laser Energy (mJ)	FWHM (deg)	D_{av} (nm)	$\delta * 10^{-2}$ $(nm)^{-2}$	$\varepsilon * 10^{-1}$
CdS Pawder	2.2133	3.6912	7.3394	5.3832
530	2.3733	3.4413	8.4440	5.7741
590	2.3800	3.4306	8.4965	5.7921
650	2.5000	3.2673	9.3672	6.0816

Figure (5) illustrates FE-SEM images of CdS NPs synthesized at various laser energies; the morphology of synthesized Nanoparticles is dependent on the laser energy. Observations indicate that the CdS nanoparticles are spherical. As depicted in Figure (5a), the average particle size of CdS nanoparticles generated with 530 mJ was approximately 23.07 nm, and aggregated particles were observed. At the laser energy was increased from 530 to 650 mJ, the nanoparticles were changed into micro and nanostructures because Increased laser energy increases the amount of laser radiation that reaches the target, hence increasing the number of NPs with a smaller size Figure (5d).

Figure (6) illustrates EDS spectra of CdS nanostructures generated at various laser energies. These spectra reveal the existence of Cd and S elements, as well as other peaks associated with

Academic Science Journal

O and C elements; these components originated from the glass substrate and liquid media. The effect of laser energy on the ratio of [Cd] to [S] is shown in Table (2).

Table 2: Elements and their weight percentage in CdS nanostructures colloidal synthesized at different laser energies

Element	CdS powder	530 mJ	590 mJ	650 mJ
Cd	**65.7**	**79.2**	**79.2**	**79.3**
S	**16.4**	**20.8**	**20.8**	**20.7**
Cd/S	**4.006**	**3.807**	**3.807**	**3.830**

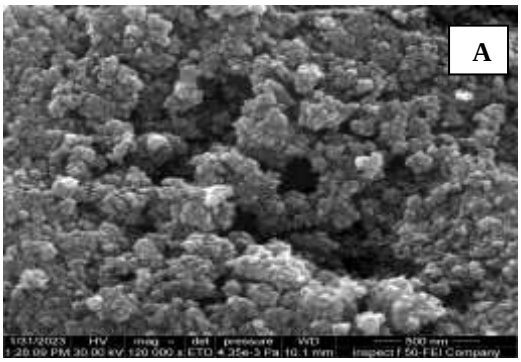

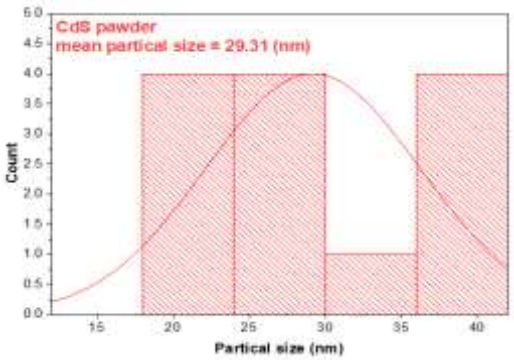

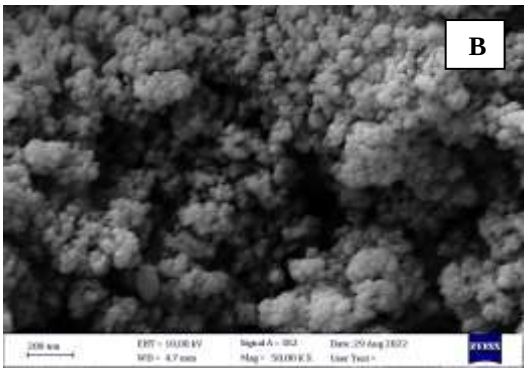

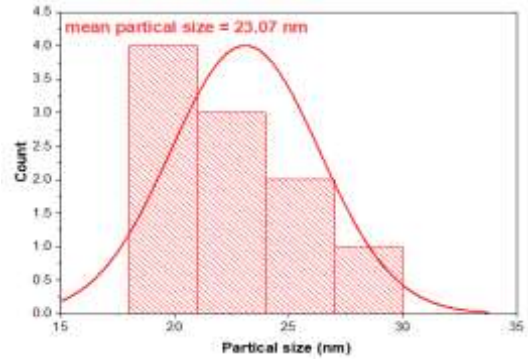

Academic Science Journal

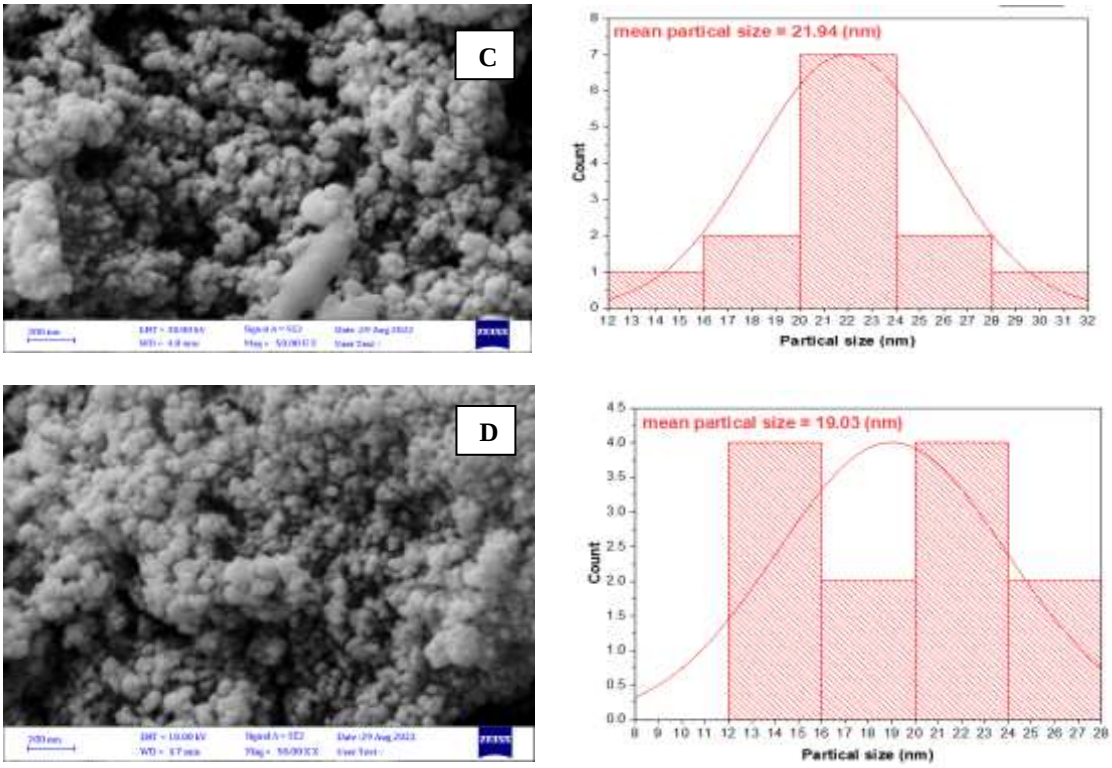

Figure 5: FE-SEM images of CdS nanoparticle synthesized at various laser energies. (A) pawder, (B) 530 mJ, (C) 590 mJ, (D) 650 mJ

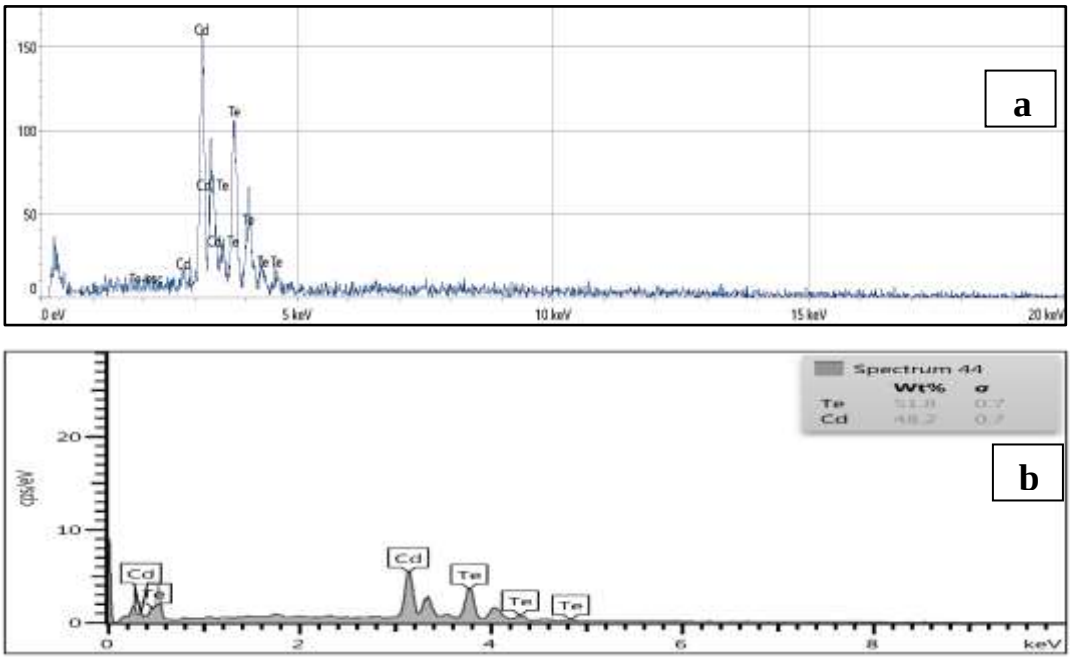

Academic Science Journal

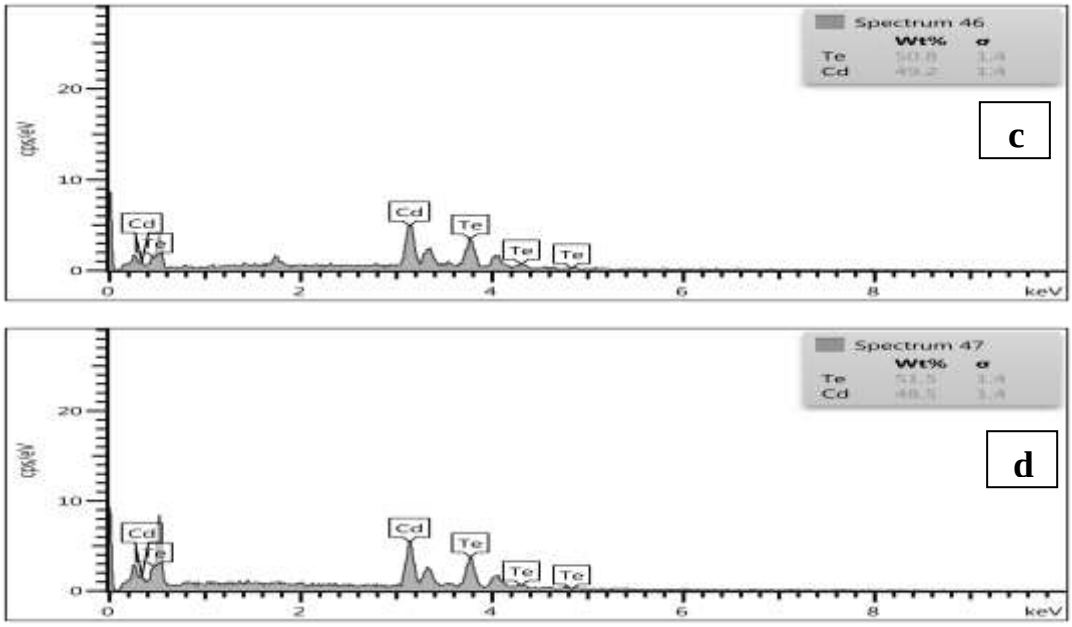

Figure 6: EDS spectra of CdS NPs synthesized at various laser energies: (a) CdS pawder, (b) 530 mJ, (c) 590 mJ, (d) 650 mJ

Analyzing the FTIR spectra Figure (7), it was discovered that the synthesized CdS nanopowder and CdS NPs synthesized with different laser energy contain a large number of absorption peaks and bands. Normally, the Cd–S stretching frequency is observed in the lower wave number range, i.e., below 700 cm^{-1} [14]. In our CdS nanoparticles, a moderately intense absorption peak at 623.689 cm^{-1} corresponding to Cd–S stretching was detected. The strong-medium and broad absorption bands at 2913.132 cm^{-1} and 1410.51 cm^{-1} have been ascribed to the O–H stretching vibration of H_2O molecules [15]. Seeing the C-O stretching at 1098 cm^{-1}. At 867.87 cm^{-1} is another modest absorption peak for O–H. C=O band is present as indicated by the peak at 1559.73 cm^{-1}. With increasing laser energy, the intensity and half-width at half-maximum (FWHM) of the absorption peaks of CdS NPs were shown to diminish significantly. The presence of respective bands and absorption peaks in the FTIR spectrum confirms the presence of CdS molecules, traces of contaminants resulting from the chemical reaction of various precursors, and hydroxide ions or water molecules in the produced nanoparticles.

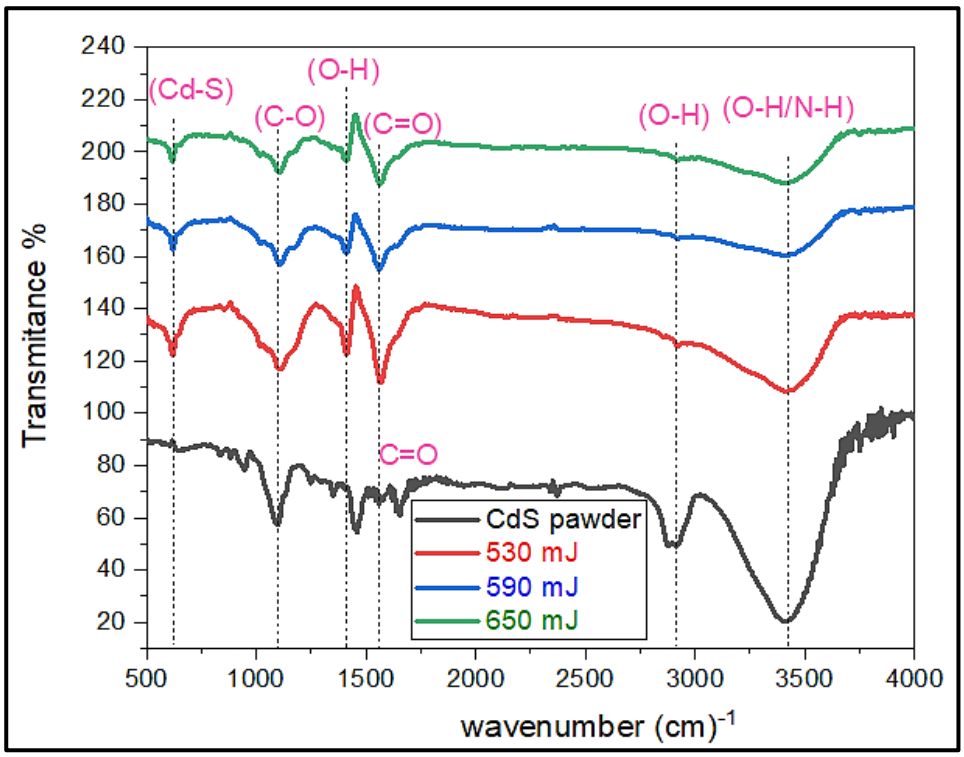

Figure 7: FTIR spectra of CdS NPs synthesized at different laser energy

c. Electrical Properties

Measuring the Hall effect was performed on CdS at (room temperature); these measurements validated the n-type conductivity of the synthesized CdS nanoparticles. Due to the decrease in sulphur to cadmium ratio, the conductivity of CdS increased from 0.1838 to 0.215 $(ohm.cm)^{-1}$ as the laser energy was increased from 530 to 650 mJ. (formation of excess interstitial cadmium ion or Sulfur vacancies represented as donor). Figures (8) and (9) show, respectively, the electron mobility (μ) and electrical conductivity (σ) of CdS nanoparticles. Due to size reduction, they show that laser energy decreases the mobility of CdS nanoparticles. At laser energy of 590 mJ, however, the mobility of CdS NPs began to increase along with the resistivity, as a result of decreased structural defects, grain size boundaries, and particle aggregation and agglomeration.

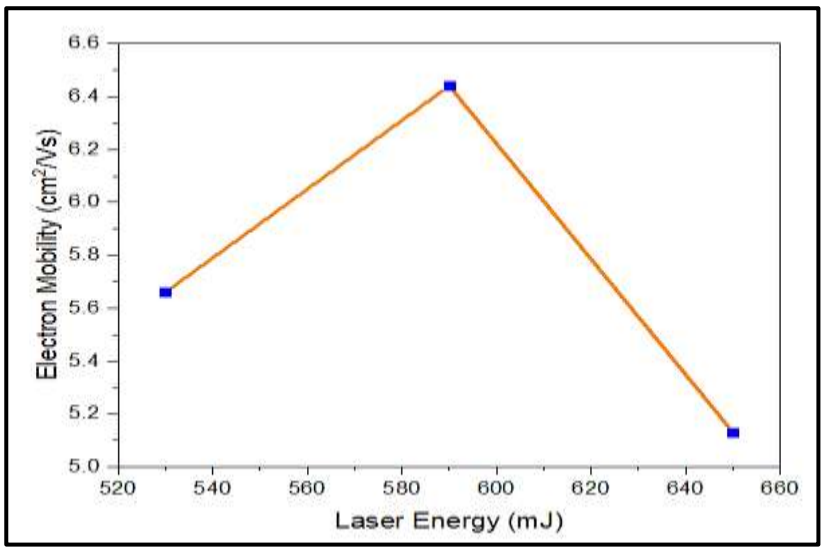

Figure 8: Electron mobility for CdS NPs prepared at various laser energies

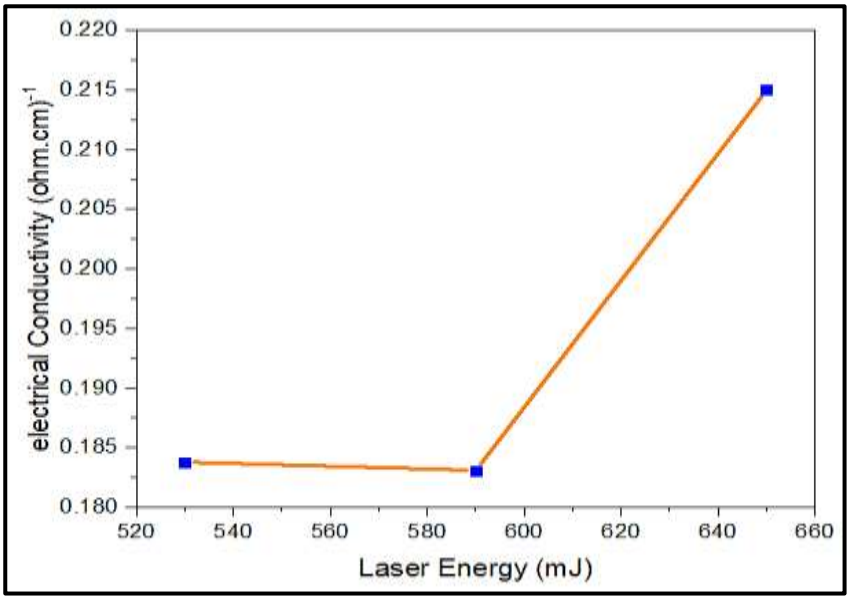

Figure 9: Electrical conductivity for CdS NPs prepared at various laser energies

Fig (10) displays the I-V characteristics of, n-CdS/p-Si under biasing (-8 V to 8 V) prepared with different laser energies. At forward bias, the current increased exponentially at increasing voltage, whereas at reverse bias, the current increased slowly at increasing voltage. No saturation or sharp breakdown was observed due to the dominance of edge leakage current which is caused by the sharp edge at the contact's periphery and the generation of excess carriers

in the depletion region. This diagram shows that heterojunctions exhibit rectification characteristics. The forward current of these photodetectors shows two distinct regions. In the first region, photodetectors will generate a small amount of recombination current when operating at low voltage. This current will be generated when an electron that has been excited from the valance band to the conduction band recombines with a hole in the valance band to restore equilibrium [16]. The second region, the forward current, also known as diffusion current, rises exponentially with increasing voltage due to the bias voltage potential exceeding the potential barriers. This biasing provides the electrons with sufficient energy to surmount the height of the barrier and flow. In addition, this diagram illustrates the laser-energy-dependent heterojunction forward characteristics. Figure (11) depicts the relationship between the rectification factor and laser energy for n-CdS/p-Si HJ. Clearly, as laser energy increases from 530 mJ to 590 mJ, the rectification factor decreases, whereas it increases as laser energy increases to 650 mJ.

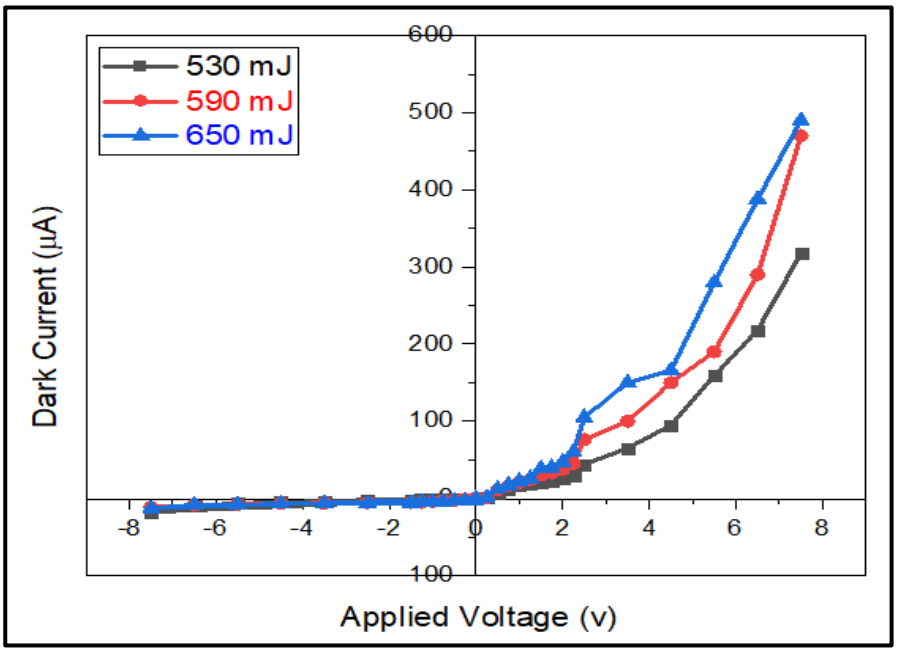

Figure 10: Dark (I-V) characteristic of n-CdS/p-Si HJ under forward and reverse bias prepared at various laser energies

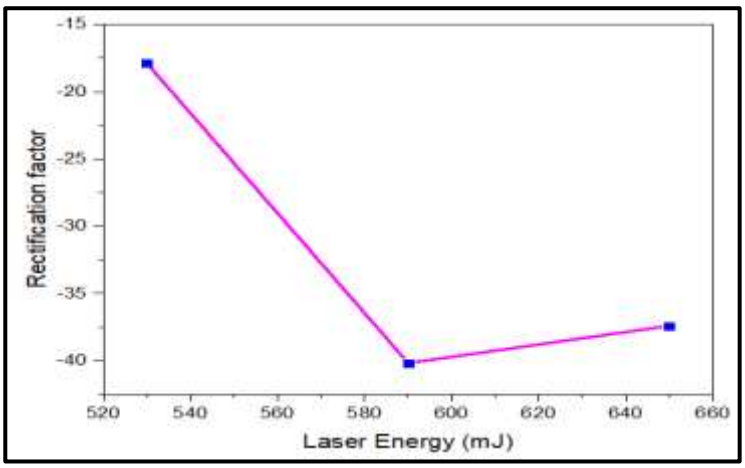

Figure 11: Variations in the rectification factor as a function of laser energy for n-CdS/p-Si photodetector

Conclusion

Using pulsed laser ablation in distilled water, hexagonal cadmium sulfide nanoparticles were effectively produced. Ablating laser energy was used to regulate the shape, size, concentration, and degree of crystallinity of nanostructured CdS. X-ray powder diffraction revealed the polycrystalline hexagonal wurtzite phase of the produced CdS nanoparticles. The (FE-SEM) analysis of produced CdS revealed hexagonal nanoparticles with a grain size of approximately 29.31 nm. The direct energy gap fluctuation of CdS (2.42-1.71 eV) and the rise in CdS optical absorption were observed to be dependent on laser energy. At room temperature, photoluminescence (PL) revealed that both the intensity of the PL emission peaks and the (FWHM) had increased.

References

1. B. Bhushan, Introduction to Nanotechnology, (Springer Handbook of Nanotechnology, 2017)
2. A. K., Ali, Preparation of Ag and Au Nanoparticles by Pulsed Laser Ablation in Liquids, Baghdad University, PhD Thesis, (2010)
3. A. K. Deniz, Gold Nanoparticle/Polymer Nanofibrous Compositesby Laser Ablation and Electrospinning, Material Letters, 65, 2941-2943(2011)

4. R. Seoudi, W. Essa, Preparation, Characterization and Physical Properties of CdS Nanoparticles with Different Sizes, Journal of Applied Sciences Research, 8, 676-685 (2012)
5. A. Dumbrava, C. Badea, G. Prodan, V. Ciupina, Synthesis and Characterization of Cadmium Sulfide Obtained at Room Temperature, 7, 111 – 118 (2010)
6. N. Qutub, Cadmium Sulphide Nanoparticles, Ph.D. Thesis, India, (2013)
7. K. Acharya, Photocurrent Spectroscopy of CdS/PLASTIC, CdS/GLASS, and ZnTe/GaAs Hetero-Pairs Formed with Pulsed-Laser Deposition, Ph. D. thesis, Bowling Green State University, (2009)
8. H. Zeng , Xi-Wen Du , Subhash C. Singh , Sergei A. Kulinich , Shikuan Yang , Jianping He, Weiping Cai, Nanomaterials via Laser Ablation/Irradiation in Liquid: A Review, Adv. Funct. Mater., 22, 1333–1353(2012)
9. N. G. Semaltianos, Nanoparticles by Laser Ablation**,** Critical Reviews in Solid State and Materials Sciences, 35,105–124(2010)
10. C. Mwolfe, N. Holouyak, G. B. Stillmau, physical properties of semiconductor, (Printice hall, New York, 1989)
11. V. Elnaz, D. Dorranian, Effect Of Ablation Environment On The Characteristics Of Graphene Nanosheets Produced By Laser Ablation, Studia Universitatis Babes-Bolyai, Chemia, 61(4), 277-284 (2016)
12. F. Ouachtari, A. Rmili, S. E. Elidrissi, A. Bouaoud, H. Erguig, P. Elies, Influence of Bath Temperature, Deposition Time and [S]/[Cd] Ratio on the Structure, Surface Morphology, Chemical Composition and Optical Properties of CdS Thin Films Elaborated by Chemical Bath Deposition, Journal of Modern Physics, 2, 1073-1082 (2011)
13. R. S. Alnaily, M. L. Sheqnab, Study the optical and structure properties of CdTe nanoparticles prepared by pulsing laser ablation in distilled water, Journal of Kufa–Physics, 11(1), (2019)

14. A. Sabah, S. Siddiqi, S. Ali, Fabrication and Characterization of CdS Nanoparticles Annealed by using Different Radiations, International Journal of Chemical and Molecular Engineering, 4, 532-539(2010)
15. N. Yogamalar, K. Sadhanandam, A. Bose, R. Jayavel, Quantum confined CdS inclusion in graphene oxide for improved electrical conductivity and facile charge transfer in hetero-junction solar cell, RSC Advances, 5, 16856-16869 (2015)
16. T. S Oktik, S. Altindal, T.S. Mammadov, Electrical characterization of novel Si solar cells, Journal of Thin Solid Films, 258, 511–512(2006)